

Chapter 10
Data-driven Wireless Positioning

Maximilian Stahlke, Tobias Feigl, Sebastian Kram, Jonathan Ott, Jochen Seitz, Christopher Mutschler

Abstract Radio-based indoor localization is a crucial enabler for various tasks like robot navigation or quality assurance in industrial assembly. However, especially industrial environments often present challenging propagation conditions, with reflections, diffraction obstruction, and blockage. While traditional, lateration-based positioning algorithms can provide high accuracies in line-of-sight (LOS) conditions, signal blockages cause non-line-of-sight (NLOS) propagation and degrade the performance dramatically. To overcome this problems, recently artificial intelligence (AI)-driven localization algorithms have shown promising results and can provide robust and high localization performance in such challenging environments. In this chapter, we evaluate the performance of AI-models trained on radio fingerprints in various challenging industrial environments. We evaluate the accuracy and the effect of environmental changes on the localization performance and robustness. Our results show that environmental changes significantly degrade the performance, which leads to a high effort in maintenance, i.e., keeping the models up-to-date. We show how to combine classical lateration-based algorithms with data-driven models employing uncertainty estimation to reduce the the effort for initial deployment and maintenance for a more robust localization solution.

Key words: indoor localization, lateration-based positioning, AI-driven localization, hybrid localization.

Fraunhofer Institute for Integrated Circuits IIS, Fraunhofer IIS, Nuremberg, Germany

Corresponding author: Maximilian Stahlke
e-mail: maximilian.stahlke@iis.fraunhofer.de

© The Author(s) 2024

C. Mutschler et al. (eds.), *Unlocking Artificial Intelligence*,
https://doi.org/10.1007/978-3-031-64832-8_10

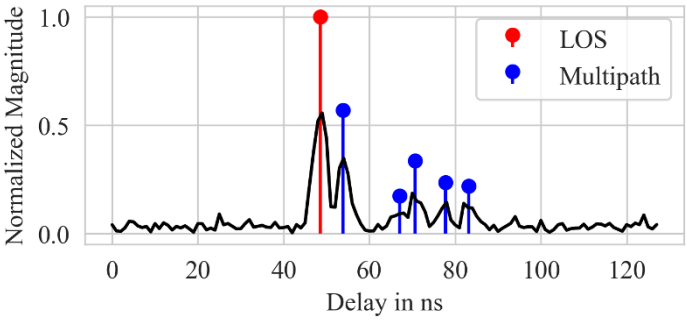


Fig. 10.1: Simulated CIR with 250 MHz bandwidth limitation. The LOS and multipath components are depicted as stems.

10.1 Introduction

Indoor positioning systems achieve reliable localization in industrial environments and enable various tasks such as process monitoring or the navigation of autonomous robots. There are methods based on cameras [13, 12], a combination of inertial sensors and cameras [14], or other modalities like LiDAR [23] and ultrasonic [23], which enable high localization accuracies. However, these methods often lack robustness due to changing light conditions, to dynamics of industrial environments, or interferences in the measured data [22, 15, 3, 7]. Therefore, radio-based localization methods are often employed providing high localization accuracies in such environments. Traditionally, methods such as lateration based on the time-difference-of-arrival (TDOA) are used to estimate positions. While these algorithms achieve localization accuracies in the decimeter range in LOS scenarios, NLOS between the receiver and the transmitter – the access point (AP) – significantly lowers the positioning accuracy. However, in realistic indoor scenarios, often a limited amount of APs is available, which often leads to areas where the minimum number of three APs in LOS cannot be ensured. To enable high localization accuracy in such NLOS dominated areas, instead of classical TDOAs, channel impulse responses (CIRs) can be used as an information source for positioning. These signals are complex time-series that are acquired through correlation with known pseudo-random pulses. They resolve all propagation components and therefore can contain a variety of spatial information.

Fig. 10.1 shows a bandwidth-limited CIR that includes a LOS component (red) as well as five additional signal components (blue). To exploit all the information contained in the high-dimensional CIR, machine learning (ML)-based methods can be used to assist radio localization systems, i.e., NLOS identification [20, 19], time-of-arrival (TOA) error mitigation [5], or multipath-assisted localization [9]. While [5, 9] consider all signal components (red and blue stems in Figure 10.1), the methods proposed by [20, 19] improve the positioning by enhancing LOS information (red

stem in Figure 10.1). However, those methods still require few APs in LOS to achieve reliable positioning. To enable localization in NLOS-dominated areas, fingerprint-based localization methods utilizing channel information, such as the bandwidth-limited CIR (black line in Figure 10.1), can be employed [11, 17, 21]. These, so-called direct positioning methods, are independent to the radio propagation conditions and thus do not require a redundant deployment of APs to ensure LOS conditions. However, their main drawback is that they need an expensive life cycle management due environmental changes, including recording and labeling of data, fine-tuning and deployment of positioning models.

In this work, we briefly review AI-assisted localization methods and focus on investigations of the robustness of AI-based direct positioning localization models at different environmental changes, i.e., moving persons or objects or (non-)deterministic LOS blockage and discuss the impact on the life cycle management. Finally, we propose an approach to combine AI models trained on radio fingerprints with traditional localization methods in order to lower the efforts for maintenance and deployment.

10.2 AI-Assisted Localization

AI-assisted localization methods combine classical localization methods, like lateration based methods, with AI models. Their idea is to mitigate errors introduced by the environment like NLOS conditions or exploit additional information, which can not be modeled analytically, like multipath information.

A promising method is to identify NLOS signals and exclude them for localization. In our previous work, we investigated different supervised and unsupervised ML approaches. We used convolutional neural networks (CNNs), which employ the CIR to identify whether a signal has LOS or NLOS [19]. Given CIRs with labels (LOS, NLOS), CNNs can effectively model the temporal correlations in the high dimensional CIR to classify the channel conditions. However, labeling NLOS signals is often challenging in real world environments. While LOS signals are similar to LOS in visible light conditions, radio signals can propagate through various materials, like cardboards or wood and thus beeing in LOS for radio signals, but not for visible light. Thus labeling NLOS signals is often challenging or not possible in certain types of environments. To overcome this problem, we proposed to only use LOS signals for a classification by modeling the distribution of LOS CIRs and identify NLOS signals as out-of-distribution samples [20]. We used a variational autoencoder to model the distribution of in-domain samples, i.e., LOS CIRs, to identify NLOS signals by its lower data likelihood. While we achieve lower accuracies compared to supervised methods, we overcome the problem for labeling NLOS signals.

Another challenge is dense multipath propagation. Due to the limited bandwidth of radio signals, multipath components (MPCs), i.e., reflections from the environment, may not reliable separated in the radio channel. Thus, also under LOS conditions the TOA measurements may be erroneous due to interference of MPCs. Also here AI

methods can be used to estimate reliable TOA estimations. We employed a CNN to estimate the TOA in a provided CIR given the true TOA [5]. We have shown that our method works even under dense multipath propagation with restricted bandwidth. Thus we could successfully mitigate the errors of interference and provide reliable TOA measurements for classical lateration based methods. However, the radio channel does not only include the first direct path of arrival (FDPOA), but also all the reflections of the environment. This information can be used by multipath-assisted positioning [6]. Their idea is to learn virtual anchors, represented by reflections of e.g. walls, and use them as additional APs. A crucial component in the learning process is a reliable MPC delay estimation. We employed a U-Net [16], well known for time series segmentation, to estimate the delays of MPC components outperforming classical sub-space methods in accuracy and inference time [9].

10.3 Direct Positioning

AI-assisted localization methods still require APs with LOS conditions to enable localization. For very complex, NLOS dominated, environments, only methods that exploit the radio fingerprint of a radio system estimate very accurate positions. Stahlke et al. [17] have shown that exploiting the channel impulse response (CIR) [2] with the corresponding time-of-arrival (TOA) can achieve high localization accuracy in complex NLOS environments en par with the performance of traditional tracking solutions under ideal LOS conditions. The idea of the data-driven approach is to train a deep learning (DL) model with a labeled dataset of channel impulse responses (CIRs), TDOAs, and the corresponding reference positions. The trained model can then, independent of the propagation conditions of the environment, predict the position utilizing channel information. However, the main disadvantages of the approach are (1) that the training database must cover fine-grained radio fingerprints of the area of interest within the environment to enable accurate localization, and (2) that the radio fingerprint, and thus the database, depend on the specific propagation environment. Hence, changes in the environment, e.g., movements of blocking objects such as cars or shelves, significantly change the fingerprint of the radio device, and consequently, lead to significant localization errors. In this work, we evaluate the performance of data-driven fingerprint-based positioning in various industrial-like environments and the effect of environmental changes on the performance of the models.

10.3.1 Model

We follow the idea of Stahlke et al. [17] to create a DL model, which exploits the raw CIR in the time-domain and the corresponding TDOA, for direct positioning. An example visualization is shown in Figure 10.2. For every burst (set of received

CIRs per timestep), for the calculation of the TDOA, the first (earliest) TOA is used. The CIRs, shown in blue on the left hand side, of all APs are horizontally stacked, while every CIR is padded by the TDOA to get a relative alignment of the signals in the input tensor of the neural network. The idea is to extract and exploit all (spatial) information of a CIR, i.e., diffractions, reflections, and absorptions, to get a unique fingerprint for every position in an environment.

Inspired by the work of Niitsoo et al. [11] we also employ CNNs as they have shown very accurate results in processing image and time-series data. However, Fawaz et al. [4] have shown, that very simple CNN architectures without local pooling can outperform highly complex models with local pooling layers in time-series applications. Hence, in contrast to the CNN of Niitsoo et al. [11], we employ a simple CNN architecture without local pooling to exploit the full information of the time-series data.

10.3.2 Experimental Setup

We used a 5G-compatible software-defined radio system with commercial of the shelf hardware. The system is a downlink TDOA system with 6 APs within an industrial hall. The system has a bandwidth of 100 MHz with a carrier frequency of 3.75 GHz (Lower bandlimit: 3.7 MHz; Upper bandlimit: 3.8 MHz). The TX Power of the APs is 20 dBm. The receiver records bursts (consecutive signals for every AP) at 100 Hz.

The hardware setup of the receiver and the distribution of the APs within the L.I.N.K. application center of Fraunhofer IIS in Nuremberg [1] are shown in Fig-

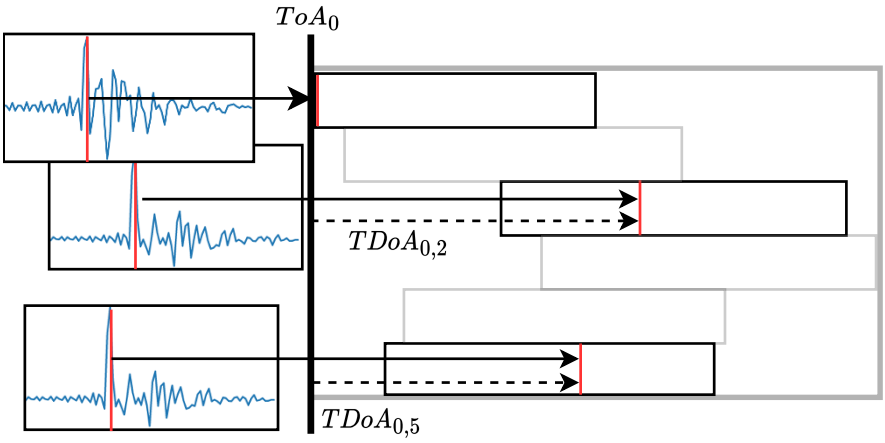
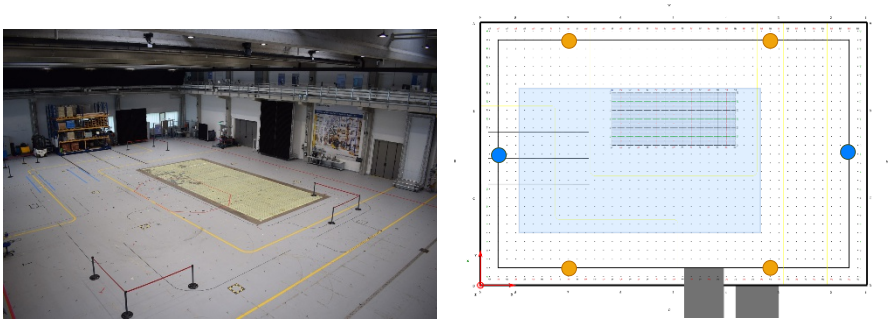
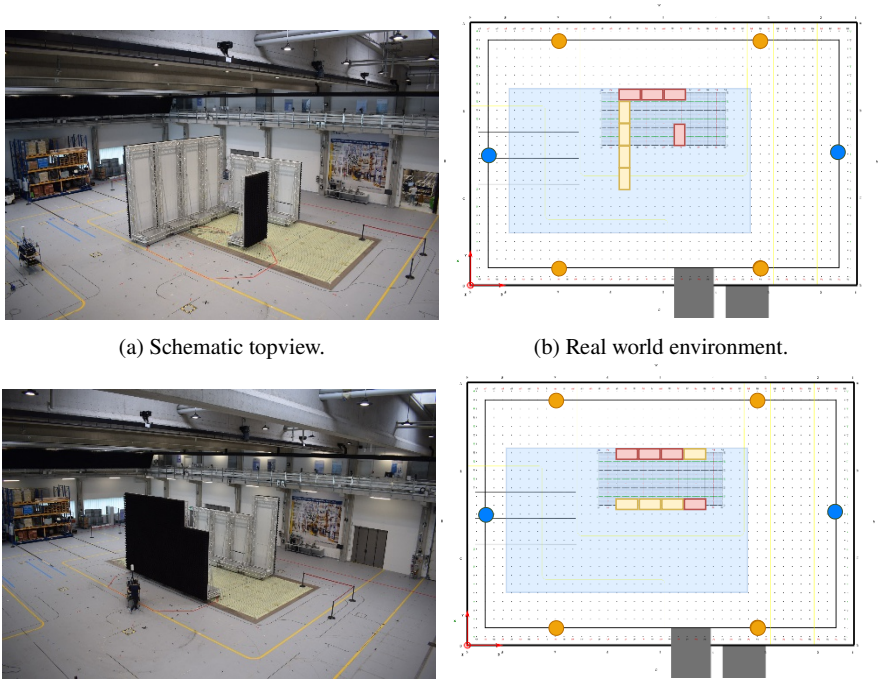


Fig. 10.2: Input embedding for the neural network. The CIRs, shown on the left hand side in blue, are aligned by their TDOA and horizontally stacked.



(a) Real world environment. (b) Schematic topview.

Fig. 10.3: LOS environment.

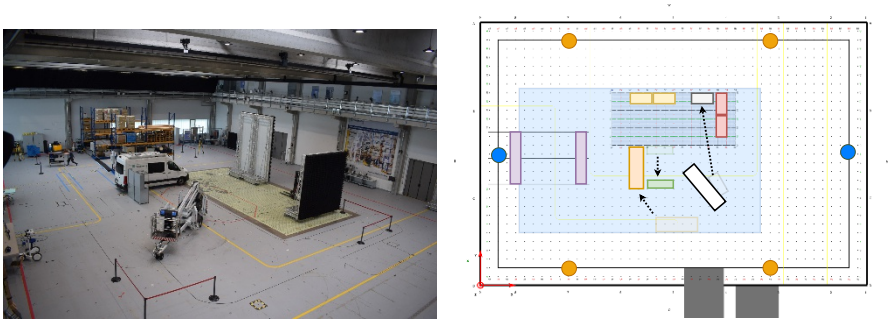


(a) Schematic topview. (b) Real world environment.

(c) Schematic topview. (d) Real world environment.

Fig. 10.4: Deterministic mixed environments with absorber L-shaped (DS1) on the top and absorber corridor (DS2) on the bottom.

ure 10.3. In total 6 APs are available, indicated as dots within the schematic top view on the left-hand side. The blue APs are placed at a height of 6.5 m, while the orange APs are placed at a height of 7.5 m.



(a) Real world environment. (b) Schematic topview.

Fig. 10.5: Realistic industrial environment with various industrial objects.

10.3.2.1 Measurement Campaign

In order to demonstrate the accuracy, robustness, and transferability of the proposed data-driven approach an extensive measurement campaign was conducted including three different types of environments. In general, all recordings took part in the L.I.N.K. hall, shown in Figure 10.3 on the left-hand side. For all environments the recording area (28 m $\times$ 18 m) remained the same. For each environment, we recorded 1 - 1.5 hours of data covering several people on random trajectories to mimic a realistic data acquisition that still covers the area of interest. With a recording frequency of 100 Hz, we therefore achieve a database size of 2-3 million CIRs per environment with 6 APs. As ground truth we used a Nikon iGPS, an optical reference system with a positioning error of $MAE < 1$ mm.

10.3.2.2 Environments

In total, six different environments were recorded to investigate the effects of various environmental changes. Figure 10.3 shows the LOS environment, while the image on the left-hand side shows the real environment and the figure on the right-hand side shows a schematic top view. It contains no obstacles, which means that all APs have LOS to the receiver rendering it ideally for traditional TDOA-based localization systems. In Figure 10.4, the environments (DS1) and (DS2) are shown. We added walls, which absorb the signals on the outside (black) and reflect them on the inside (metal). In this environments we created severe NLOS conditions blocking the LOS to almost the half of the APs all the time. Due to the different composition of the absorber walls, the fingerprints are different at almost every position rendering a good candidate for a cross environment evaluation.

The last environments are shown in Figure 10.5. We created a typical industrial environment (RS1) with various objects, like a forklift, a van, metal shelves, and a working platform. We introduced realistic changes (RS2), where we moved the

van, added an additional work platform, and moved the forklift (3C). Those changes should reflect realistic changes of a dynamic industrial environment. More details about the environments and its changes can be found in [17].

10.3.3 Evaluation

We trained our models in all of the environments and conducted a cross validation, i.e., tested them in the same and in the other environments. The results can be seen in Table 10.1, i.e. mean absolute error (MAE) on the left and the 90th percentile of the cumulative distribution function of the absolute error (CE_{90}) on the right. The models are trained and tested in all environments to see the impact of the environmental change. The diagonal elements show the results, where the model is trained and tested in the same environment, while the off-diagonal elements show the results, where the models are trained and tested in different environments. In general, the performance is high for all environments, with a $CE_{90} < 0.7$ m for all scenarios. The positioning accuracy is the lowest in the LOS environment compared to the other mixed environments. Under LOS conditions the CIR contains less information about the environment, as only few multipath components are present (e.g., floor or ceiling) compared to mixed environments with dense multipath like in the corridor environment (DS2). However, in the other environments the positioning accuracy is very high. The performance degrades for the model in a different composition of the environment, as the radio fingerprint changes due to different multipath propagation and changes of the channel state (i.e., LOS to NLOS and vice versa). If the model is trained in the LOS environment and tested in a mixed scenario, the performance degrades with a $CE_{90} > 2$ m for all environments. This is due to the different propagation conditions for the area. Dense multipath and different channel states (LOS / NLOS) cause changed radio fingerprints, and therefore, lead to a degrading positioning accuracy. If the model is trained in the initial industrial environment (RS1) and evaluated in the changed industrial scenario (RS2), the positioning performance degrades only slightly. This is due to the fact that the environment only changed slightly, which leads to only local anomalies.

Table 10.1: Position accuracy and robustness of our model against various environmental changes (MAE | CE_{90} in [m]).

		Evaluated									
		LOS		DS1		DS2		RS1		RS2	
Trained	LOS	0.41	0.68	1.24	2.50	1.71	3.90	1.42	3.00	1.40	2.87
	DS1	1.23	2.22	0.34	0.61	1.54	2.75	2.01	4.00	1.99	3.90
	DS2	1.18	2.16	1.32	2.65	0.26	0.49	1.84	3.59	1.84	3.76
	RS1	0.83	1.59	1.50	2.78	1.21	2.17	0.32	0.58	0.49	0.92
	RS2	1.05	1.89	1.50	2.93	1.20	2.21	0.48	0.92	0.35	0.61

10.3.4 Hybrid Localization

As shown in Section 10.3.3, data-driven models are affected by environmental changes and need a life cycle management to ensure reliable localization. The effort increases with the size of the environment, as the new data has to be recorded and labeled for all changed areas. However, indoor environments are often heterogeneous, which means that there are sections which are dominated by NLOS, while some areas still have enough LOS to enable traditional positioning.

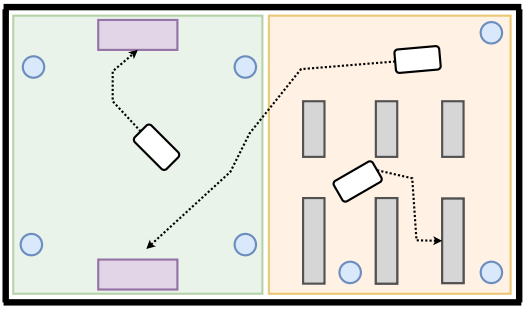
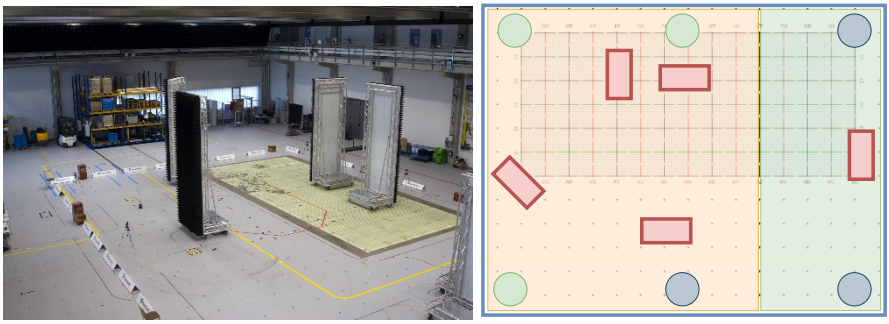


Fig. 10.6: Schematic top view of a typical (dynamic) industrial environment with an ultra-wideband localization system.

Figure 10.6 represents a typical industrial environment, with shelves with goods (grey rectangles) and machines (purple rectangles). An ultra-wideband (UWB) radio system is deployed, shown as blue circles, to localize automated guided vehicles (AGVs), indicated as white rectangles. The area is separated in two sections with different complexities for localization. For the localization in the left area, a machine hall (green), traditional localization approaches can be employed as there is always LOS to at least four transmitters. In contrast, the area on the right-hand side, the LOS is blocked to the majority of the transmitters. To still achieve high localization accuracies, data-driven models have to be deployed, with the overhead for an expensive life cycle management. To enable a cost-efficient, continuous, and robust localization, a combination of AI based and traditional localization methods is needed, which requires the identification of the spatial limitation of the data-driven positioning model.

10.3.5 Zone Identification

To identify the spatial limitation of our data-driven model, we employ the method proposed by Stahlke et al. [18]. Their idea is to model the epistemic uncertainty [8] of the AI model to identify out-of-distribution samples. In fingerprint-based localization, we assume that the received signals are unique for a certain position, as the received signals only depend on the environment. We record the data in the training



(a) Real world environment. (b) Schematic topview.

Fig. 10.7: Realistic industrial environment with heterogeneous zones for localization.

area with a high spatial density to ensure that new recordings within the training area are already covered. Thus, the neural network is confident about unseen data within the training area and predicts a low epistemic uncertainty. In contrast, samples recorded outside the training area are different to all recorded samples within the training area. This leads to a high epistemic uncertainty of the neural network, which helps us to identify the spatial limitation of the model. We employed the probabilistic ensemble [10], with a neural network architecture very similar to the one used in Section 10.3.1. More details about the implementation and architecture can be read in [18]. To identify samples, which are outside of the training area, a threshold has to be defined for the uncertainty to detect samples within and outside the training data distribution. Methods like interquartile ranges could be used to detect out-of-distribution samples. However, they might require some fine-tuning. To ensure a reliable threshold, we used a logistic regression classifier, which uses few samples out-of and inside-of the training area.

10.3.6 Experimental Setup

For the evaluation, a UWB radio system with six stationary transceivers is employed with one dynamic transceiver carried by a small robot platform. The system is configured to estimate the round-trip-time (RTT) at the robot platform with a bandwidth of 499.2 MHz at a center frequency of 4 GHz. The recorded data is labeled with an optical ground truth reference system with a recording frequency of 4 Hz.

10.3.7 Environments

Also in this experiment, we created an industrial-like environment including walls, which absorb radio signals on the outside (black) and reflect them on the inner side. The environment is shown in Figure 10.7, where the real-world environment is on the left-hand side and the schematic top view is on the right-hand side. The stationary transceivers are indicated as dots and are placed on the upper and lower part of the recording area. The reflective walls are indicated in red and are placed to block the LOS between the stationary transceivers and the moving robot, which causes ranging errors and thus also to a degradation in the localization performance with traditional positioning approaches. The environment is separated into two areas: The left area (orange), is very cluttered and mostly dominated from NLOS to the transceivers, while the right area (green) is more open and provides always LOS to the transceivers indicated in grey.

10.3.8 Evaluation

The uncertainty, estimated by our probabilistic ensemble, can be seen in Figure 10.8. The dashed black line separates the training area (left) and the unseen area (right). It can clearly be seen that the uncertainty identifies the spatial limitations of the direct

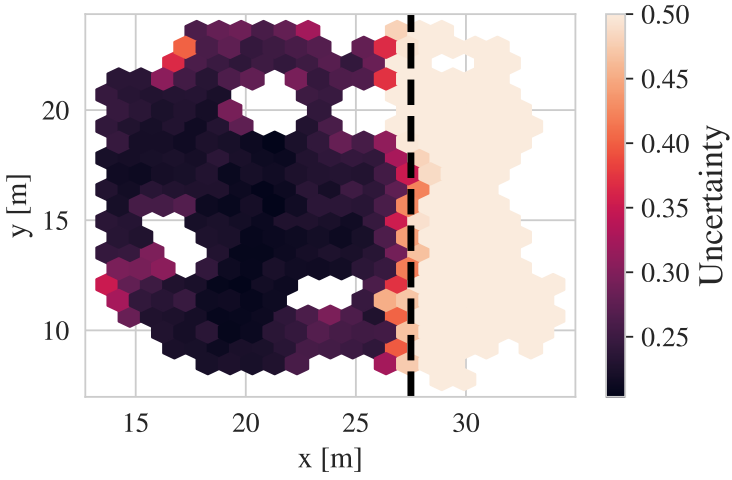


Fig. 10.8: Spatial distribution of the uncertainty of our probabilistic ensemble. The dashed black line indicates the transition from the training area (left) to the unseen area (right).

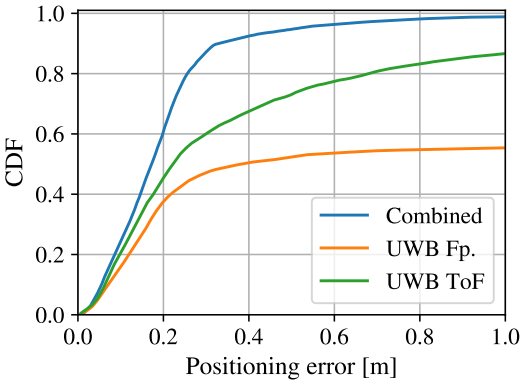


Fig. 10.9: CDFs of the errors for the fingerprint based model (UWB Fp.), the classical localization model (UWB ToF) and our proposed combined model (Combined).

positioning model very well. The data in the training area has a low uncertainty (black) compared to the samples out of the training data area (red). The decision boundary is very sharp, which means that an identification is feasible with the proposed approach.

To combine traditional localization methods with data-driven, fingerprint-based, methods, we use a Kalman filter. While the uncertainty is low, the positions of the model are fed to the Kalman filter. However, if the uncertainty rises above an uncertainty threshold, the distance estimations of only the three transceivers on the right hand side (grey), shown in Figure 10.7, are fed to the tracking filter as they have LOS in the area on the right hand side. The errors of the localization are shown in Figure 10.9, using only traditional positioning (UWB ToF), only data-driven positioning with the model trained on the left hand side (UWB Fp.) and the fusion of data-driven and traditional localization (Combined). It can clearly be seen that the data-driven method only works in 50% of the cases. Thus, the error is up to a MAE of of 2.72 m and a CE_{90} of 8.46 m. The model is only trained on the left hand side, see Figure 10.7 in orange, and can not extrapolate into the right hand side. Hence, the error on the right hand side is very high. If only the traditional positioning is used, the MAE is at 0.56 m and the CE_{90} at 1.39 m. NLOS causes errors in the distance estimations, which leads to a degradation of the positioning results. The best results can be achieved with the combined approach with a MAE of 0.21 m and a CE_{90} of 0.32 m. The data-driven model ensures robust localization in the cluttered left hand side area, while the traditional localization takes over on the right hand side. The evaluations have shown that a combination of both approaches is therefore useful to lower the effort for data recording and maintenance. To enable this, an explicit identification of the spatial limitation of the data-driven models is crucial to ensure reliable and robust positioning.

10.4 Conclusion and Outlook

In this work, we have successfully shown that AI can enhance the accuracy of radio localization systems in complex indoor environments. However, to enable a robust and reliable positioning an expensive life-cycle-management has to be employed. In an extensive ablation study, including 5 different scenarios, we evaluated that data-driven models trained on radio fingerprints cannot generalize to different environments and various environmental changes. While indoor environments often provide heterogeneous areas, with sections fully dominated by NLOS and more open areas with sufficient numbers of LOS connects. A combination of classical localization methods and data-driven methods is therefore useful to lower the expenses for maintenance and still achieve overall high localization accuracy.

We have shown how to combine traditional localization and data-driven localization based on radio fingerprints by uncertainty estimation. This allows us to identify the spatial limitations of the data-driven methods, which allows us to only employ the data-driven models in NLOS dominated areas, while classical positioning can be used elsewhere. This lowers the risk of out-dated radio fingerprints and the expenses for labeling and maintenance.

One potential avenue for future research involves the mitigation of the high cost associated with labeling extensive datasets. Addressing this challenge may entail exploring unsupervised or self-supervised learning methodologies, which hold promise in minimizing the dependency on labeled data points. Additionally, an ongoing inquiry pertains to the integration of fundamental physical principles, such as Maxwell's equations, into data-driven methodologies. Incorporating such knowledge has the potential to enhance the generalization abilities of these methodologies while concurrently diminishing the requisite volume of data.

Acknowledgements

We thank Maximilian Kasparek, Andreas Eidloth, Jan Niklas Bauer and Mohamed Soliman for implementing the proof-of-concept 5G uplink-TDOA positioning setup and its software-defined-radio-based processing pipeline.

References

1. L.I.N.K. application center of Fraunhofer IIS. https://www.iis.fraunhofer.de/de/profil/standorte/linkhalle.html.
2. T. Altstidl, S. Kram, O. Hermann, M. Stahlke, T. Feigl, and C. Mutschler. Accuracy-Aware Compression of Channel Impulse Responses Using Deep Learning. In *IEEE Intl. Conf. on Indoor Positioning and Indoor Navigation (IPIN)*, Lloret de Mar, Spain, Nov. 2021.
3. T. Brieger, N. L. Raichur, D. Jdidi, F. Ott, T. Feigl, J. R. van der Merwe, A. Rügamer, and W. Felber. Multimodal Learning for Reliable Interference Classification in GNSS Signals. In

Proc. of the Intl. Technical Meeting of the Satellite Division of the Institute of Navigation (ION GNSS+), pages 3210–3234, Denver, CO, Sept. 2022.
4. H. I. Fawaz, G. Forestier, J. Weber, L. Idoumghar, and P. A. Muller. "Deep learning for time series classification: a review". *Data Min. Knowl. Discov.*, 33(4):917–963, 2019.
5. T. Feigl, E. Eberlein, S. Kram, and C. Mutschler. Robust ToA-Estimation Using Convolutional Neural Networks on Randomized Channel Models. In *IEEE Intl. Conf. on Indoor Positioning and Indoor Navigation (IPIN)*, Lloret de Mar, Spain, Nov. 2021.
6. C. Gentner, T. Jost, W. Wang, S. Zhang, A. Dammann, and U.-C. Fiebig. Multipath assisted positioning with simultaneous localization and mapping. *IEEE Transactions on Wireless Communications*, 15(9):6104–6117, 2016.
7. D. Jdidi, T. Brieger, T. Feigl, D. C. Franco, J. R. van der Merwe, A. Rügamer, J. Seitz, and W. Felber. Unsupervised Disentanglement for Post-Identification of GNSS Interference in the Wild. In *Proc. of the Intl. Technical Meeting of the Satellite Division of the Institute of Navigation (ION GNSS+)*, pages 1176–1208, Denver, CO, Sept. 2022.
8. A. Klaß, S. M. Lorenz, M. W. Lauer-Schmaltz, D. Rügamer, B. Bischl, C. Mutschler, and F. Ott. Uncertainty-aware Evaluation of Time-Series Classification for Online Handwriting Recognition with Domain Shift. In *IJCAI-ECAI Intl. Workshop on Spatio-Temporal Reasoning and Learning (STRL)*, volume 3190, Vienna, Austria, July 2022.
9. S. Kram, C. Kraus, M. Stahlke, T. Feigl, J. Thielecke, and C. Mutschler. Delay Estimation in Dense Multipath Environments Using Time Series Segmentation. In *IEEE Wireless Communications and Networking Conference (WCNC)*, Apr. 2022.
10. B. Lakshminarayanan, A. Pritzel, and C. Blundell. Simple and scalable predictive uncertainty estimation using deep ensembles. In *Advances in neural information processing systems*, volume 30, Long Beach, California, 2017.
11. A. Niitsoo, T. Edelhäußer, E. Eberlein, N. Hadaschik, and C. Mutschler. "A Deep Learning Approach to Position Estimation from Channel Impulse Responses". *Sensors*, 19(5):1064–1091, 2019.
12. F. Ott, T. Feigl, C. Löffler, and C. Mutschler. ViPR: Visual-Odometry-aided Pose Regression for 6DoF Camera Localization. In *Proc. of the IEEE/CVF Intl. Conf. on Computer Vision and Pattern Recognition Workshops (CVPRW)*, pages 187–198, Seattle, WA, June 2020.
13. F. Ott, L. Heublein, D. Rügamer, B. Bischl, and C. Mutschler. Fusing Structure from Motion and Simulation-Augmented Pose Regression from Optical Flow for Challenging Indoor Environments. In *arXiv preprint arXiv:2304.07250 [cs.CV]*, Apr. 2023.
14. F. Ott, N. L. Raichur, D. Rügamer, T. Feigl, H. Neumann, B. Bischl, and C. Mutschler. Benchmarking Visual-Inertial Deep Multimodal Fusion for Relative Pose Regression and Odometry-aided Absolute Pose Regression. In *arXiv preprint arXiv:2208.00919 [cs.CV]*, Aug. 2022.
15. N. L. Raichur, T. Brieger, D. Jdidi, T. Feigl, J. R. van der Merwe, B. Ghimire, F. Ott, A. Rügamer, and W. Felber. Machine Learning-assisted GNSS Interference Monitoring Through Crowdsourcing. In *Proc. of the Intl. Technical Meeting of the Satellite Division of the Institute of Navigation (ION GNSS+)*, pages 1151–1175, Denver, CO, Sept. 2022.
16. O. Ronneberger, P. Fischer, and T. Brox. U-net: Convolutional networks for biomedical image segmentation. In *Medical Image Computing and Computer-Assisted Intervention–MICCAI 2015: 18th International Conference, Munich, Germany, October 5-9, 2015, Proceedings, Part III 18*, pages 234–241. Springer, 2015.
17. M. Stahlke, T. Feigl, M. H. C. García, R. A. Stirling-Gallacher, J. Seitz, and C. Mutschler. Transfer learning to adapt 5g ai-based fingerprint localization across environments. In *2022 IEEE 95th Vehicular Technology Conference: (VTC2022-Spring)*, pages 1–5, 2022.
18. M. Stahlke, T. Feigl, S. Kram, B. M. Eskofier, and C. Mutschler. Uncertainty-based fingerprinting model selection for radio localization. In *2023 IEEE 13th International Conference on Indoor Positioning and Indoor Navigation (IPIN)*, pages 1–5, 2023.
19. M. Stahlke, S. Kram, C. Mutschler, and T. Mahr. Nlos detection using uwb channel impulse responses and convolutional neural networks. In *2020 International Conference on Localization and GNSS (ICL-GNSS)*, pages 1–6, 2020.

20. M. Stahlke, S. Kram, F. Ott, T. Feigl, and C. Mutschler. Estimating ToA Reliability with Variational Autoencoders. In *IEEE Sensors Journal*, volume 22(6), pages 5133–5140, Mar. 2022.
21. M. Stahlke, G. Yammine, T. Feigl, B. M. Eskofier, and C. Mutschler. Indoor Localization With Robust Global Channel Charting: A Time-Distance-Based Approach. In *IEEE Trans. on Machine Learning in Communications and Networking*, volume 1, pages 3–17, Mar. 2023.
22. J. R. van der Merwe, D. C. Franco, J. Hansen, T. Brieger, T. Feigl, F. Ott, D. Jdidi, A. Rügamer, and W. Felber. Low-Cost COTS GNSS Interference Monitoring, Detection, and Classification System. In *MDPI Sensors*, volume 23(7), 3452, Mar. 2023.
23. R. W. Wolcott and R. M. Eustice. Fast lidar localization using multiresolution gaussian mixture maps. In *2015 IEEE international conference on robotics and automation (ICRA)*, pages 2814–2821. IEEE, 2015.

Open Access This chapter is licensed under the terms of the Creative Commons Attribution 4.0 International License (http://creativecommons.org/licenses/by/4.0/), which permits use, sharing, adaptation, distribution and reproduction in any medium or format, as long as you give appropriate credit to the original author(s) and the source, provide a link to the Creative Commons license and indicate if changes were made.

The images or other third party material in this chapter are included in the chapter's Creative Commons license, unless indicated otherwise in a credit line to the material. If material is not included in the chapter's Creative Commons license and your intended use is not permitted by statutory regulation or exceeds the permitted use, you will need to obtain permission directly from the copyright holder.

